Science Press

Trans. Nonferrous Met. Soc. China 17(2007) s295−s299

Transactions of Nonferrous Metals Society of China

www.csu.edu.cn/ysxb/

High cycle fatigue and fracture behavior of 2124-T851 aluminum alloy

LI Xue(李　雪)[1], YIN Zhi-min(尹志民)[1], NIE Bo(聂　波)[1, 2],
ZHONG Li(钟　利)[1, 2], PAN Qing-lin(潘清林)[1], JIANG Feng(姜　锋)[1]

1. School of Materials Science and Engineering, Central South University, Changsha 410083, China;
2. Northeast Light Alloy Co.Ltd., Harbin 150060, China

Received 15 July 2007; accepted 10 September 2007

Abstract: The high cycle fatigue properties and fracture behavior of 2124-T851 aluminum alloy were investigated roundly, including the fatigue crack growth rate, fracture toughness and fatigue *S*—*N* curve. Furthermore, the fatigue crack growth rate was analyzed by fitting the curves. And the microstructure of the alloy was studied using by optical microscopy, transmission electron microscopy and X-ray diffractometry, scanning electron microscopy. The results show that the fatigue strength and the fracture toughness of 2124-T851 thick plate are 243 MPa and 29.6 MPa·m$^{1/2}$ at room temperature and R=0.1, respectively. At high cycle fatigue condition, the characteristics of fatigue facture were observed obviously. And the higher the stress amplitude, the wider the space between the fatigue striations, the faster the rate of fatigue crack developing and going into the intermittent fracture area and the greater the ratio between the intermittent fracture area and the whole fracture area.

Key words: fatigue strength; fracture toughness; fatigue fractograph; 2124 aluminum alloy

1 Introduction

The 2124 aluminum alloy is widely used for aerospace and aviation, because of the relatively high strength, good corrosion resistance, heat stability and fracture toughness, and is one of the lightmass structural material[1−3]. The primary use of 2124-T851 aluminum alloy thick plate is for aerospace vehicles structure[4], such as machined fuselage bulkheads and wing skins in high-performance military aircraft. The service environment requires the material to have good fatigue resistance besides high strength, tenacity and corrosion resistance. A large number of researches[5−9] on the composition, microstructure and properties of the 2124 aluminum alloy have been reported already, as well as a few studies on its fatigue properties. SRIVATSAN et al[10] have investigated the low cycle fatigue properties of 2124 aluminum alloy. And KUNG et al[11] have studied the fatigue crack initiation and microcrack growth in 2124-T4 aluminum alloy by comparing with 2024-T4 aluminum alloy. It is found that the influence of grain size on the fatigue properties is related to the stress amplitude. And ROBIN et al[12] have investigated the fatigue crack growth retardation in 2124-T351 aluminum alloy, the result show that the crack retardation near the surface of the specimen is greater than in the plane strain region near the center. However, till now the fatigue property of 2124-T851 aluminum alloy thick plate has not been studied adequately yet. In this paper, the authors present and discuss the fatigue and fracture characteristics of aluminum alloy 2124-T851 with thickness of 30 mm, and the fracture behavior of 2124-T851 aluminum alloy was studied, in order to providing available experiment data for the engineering application of this alloy plate.

2 Materials and experimental

2124-T851 aluminum alloy was provided as a 30 mm thick plate used in this work. The chemical composition of the alloy is listed in Table 1.

Table 1 Chemical composition of studied alloy (mass fraction,%)

Cu	Mg	Mn	Fe	Si
4.22	1.40	0.56	0.20	0.12
Cr	Ti	Zn	Al	
＜0.05	＜0.12	＜0.25	Bal.	

Foundation item: Project (2005CB623705) supported by the National Basic Research Program of China
Corresponding author: LI Xue; E-mail:zurich_1@163.com

The authors mainly investigated the fatigue behavior of the as-received 2124-T851 alloy along the lengthwise direction. The fatigue crack developing rate tests, conforming to specifications in GB/T6398—2000, were performed on the MTS 810−50 kN machine, conducted at a constant, cyclic frequency of 10 Hz, stress ratio of 0.1 and maximum load of 10 kN, and the stress axes of the specimens were perpendicular to the rolling direction. The fracture toughness tests, conforming to specifications in HB5142—96, were performed on the MTS810—100 kN machine, and the stress axes of the specimens were perpendicular to the rolling direction. The axial stress fatigue samples at the gage section measured 64 mm in length and 22 mm in diameter. 3−4 samples were prepared for each testing point. The axial stress fatigue tests, conforming to specifications in HB5287—96, were performed on the JXG−100 machine, conducted at different stress amplitude of 230, 250, 270, 300, 320, 350 and 400 MPa, respectively, at a stress ratio($R=\sigma_{min}/\sigma_{max}$) of 0.1, stress concentration factor K_t of 1 and sine loading mode, and the stress axes of the specimens were parallel to the rolling direction.

In order to investigate the fatigue behavior of the 2124-T851 aluminum 30-mm-thick plate in depth, first, the initial microstructure of the as-received 2124-T851 alloy plate was characterized by optical microscopy after specimen preparation by standard metallography and polishing techniques. Second, the component of the as-tested alloy was examined by the X-Ray diffraction (XRD) analysis on D/Max 2500. Finally, fracture surfaces of the failed specimens in axial stress fatigue test were examined in a scanning electron microscope (SEM) to determine the predominant macroscopic fracture mode and to characterize the features on the fatigue fracture surface.

3 Results and discussion

3.1 Fatigue crack developing rate and fracture toughness of studied alloy

The relationship between the fatigue crack developing rate and the stress intensity factor D-value of the aluminum alloy 2124-T851 30 mm-thick plate is shown in Fig.1. The result shows that the curves of fatigue crack growth rate can be divided into three regions obviously [13], and each region corresponds to a stage of fatigue respectively, including crack initiation, slow stable crack growth and rapid fracture. The intersecting point between elongation line of curve in Region I and abscissa axis indicates the threshold value of fatigue crack, which is got as 6.5 MPa·m$^{1/2}$ approximately. When the ΔK reaches 11−12 MPa·m$^{1/2}$, the fatigue crack develops into the second stage, and the rate of crack growth changes roughly linearly with a change in stress intensity fluctuation. The low rate of slope means that the steps of crack propagation increases slowly with the increase of ΔK. When the ΔK reaches 29−30 MPa·m$^{1/2}$, the fatigue crack develops into the third stage. It can be known from the Region III that the rate of crack growth changes roughly linearly also, but the rate of slope is greater than the one of Region II. So the fatigue crack develops into the third stage, and small increases in the stress intensity amplitude produce relatively large increases in crack growth rate since the material approaches the unstable fracture.

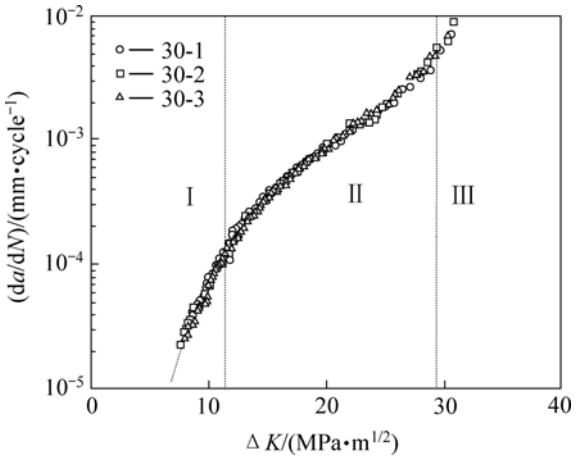

Fig.1 Curves of fatigue crack growth rate for samples

Analyzing the results of fatigue crack developing rate, the Paris formula[13], as shown in Eqn.(1), was used. A and n are parameters correlated with the material. The fitted results are shown in Table 2. It indicates that, the fatigue crack developing rate at the initiation stage is not much different from the one at slow stable crack growth stage. But when the crack developed into the rapid fracture stage, the rate increased suddenly.

$$\mathrm{d}a/\mathrm{d}N = A(\Delta K)n \quad (1)$$

Table 2 Fitted parameters for curves in Fig.1 by equation $\lg y = \lg A + n\lg x$, in which $y = \mathrm{d}a/\mathrm{d}N$, $x = \Delta K$

ΔK/(MPa·m$^{1/2}$)	lg A	n	R
＜10.11	−7.91	3.75	0.996
10.11−27.09	−7.55	3.45	0.998
27.09−30.93	−14.53	8.35	0.980

The results of fracture toughness test are shown in Table 3. The fracture toughness K_{IC} of this as-received alloy is about 29.6 MPa·m$^{1/2}$. This indicates that the value of K_{IC} corresponds to the ΔK when fatigue crack developed into the third stage. The stress intensity factor K_I increased with the crack propagation. When the crack reached a certain length, in which time the value of K_I equaled the critical stress intensity factor K_{IC}, the fatigue crack developed into the rapid fracture stage. K_{IC} means

the ability of resisting the fatigue crack unstable propagation for a specimen containing cracks, and the experimental results proves it exactly.

Table 3 Fracture toughness of 2124-T851 aluminum alloy plate

Sample No.	K_{IC}/ (MPa·m$^{1/2}$)	Mean of K_{IC}/ (MPa·m$^{1/2}$)
30-1	29.8	
30-2	29.9	29.6
30-3	29.3	

3.2 *S*—*N* curve of studied alloy

The curve of stress amplitude vs number of cycles to failure (*S*—*N*) of the studied alloy is shown in Fig.2. It can be seen from Fig.2 that first, the fatigue life of the alloy is shortened with increasing stress amplitude, for example, the fatigue life of the studied alloy is 1.0×10^7 under the stress amplitude of 250 MPa, while about 4.1×10^5 under the stress amplitude of 400 MPa. Second, from the trend of *S*—*N* curve, the fatigue lives of this alloy almost all achieve the magnitude of 10^7, when the stress amplitude was lower than 240 MPa. Therefore, through the calculation in Eqn.(2)[14], the fatigue strength of the 2124-T851 aluminum alloy 30 mm-thick plate at 10^7 cycles is 243 MPa. And third, the values of fatigue life are a little scattered under the same stress condition, for instance, the mean fatigue life of the alloy is about 6×10^6 under the stress amplitude of 250 MPa, but the best one is more than 1.0×10^7.

$$\sigma_{R(N)}=\frac{1}{m}\sum_{i=1}^{5}v_i\sigma_i=$$
$$\frac{2\times230+4\times240+3\times250+1\times260}{10}=243\ \text{MPa} \qquad (2)$$

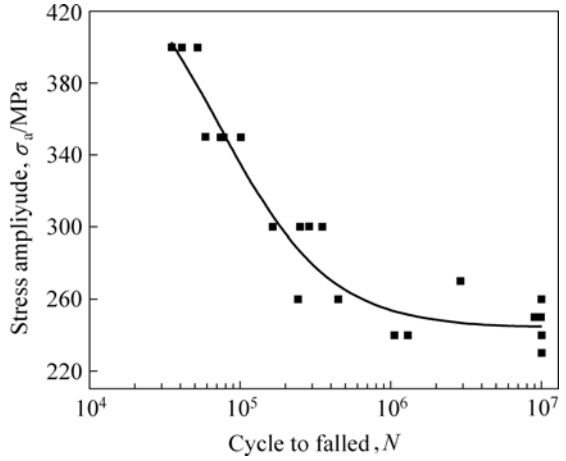

Fig.2 *S*—*N* curve for 2124-T851 aluminum alloy plane

3.3 Microstructure characterization

The microstructure of the as-received aluminum alloy is as shown in Fig.3, it can be seen from Fig.3 that the grain structure of the rolled plate is in the three orthogonal directions. The TEM images of the tested alloy are shown in Fig.4, and the XRD result is shown in Fig.5.

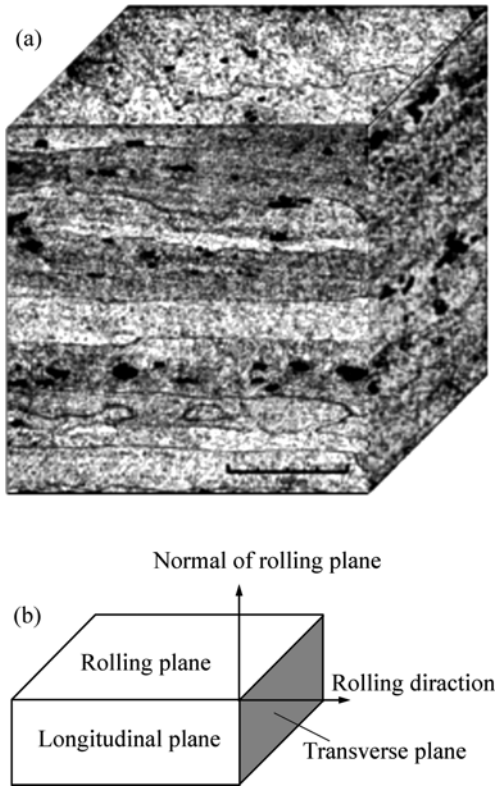

Fig.3 Triplanar optical microscope of 2124-T851 aluminum alloy plane with 30 mm thickness: (a) Result of triplanar optical microscope; (b) Orientation of Fig.4(a)

Fig.3 shows that the grain of the specimen is pancake-like, and the microstructure is partially recrystallized, with fairly large recrystallized grains that are elongated in the longitudinal direction as a consequence of deformation during rolling.

The results in Figs.4 and 5 show that 2124-T851 aluminum alloy is composed of solid solution matrix, dislocation substructure with spot-like precipitated phase *S*′(Al_2CuMg) and Al6(Fe, Mn) particles, a few of Al6(Fe, Mn) are coarse particles. It can be seen in the subsequent SEM fractograph that such phases would cleavage fracture during the process of fatigue fracture, and this was detrimental to the fatigue properties of the alloy [15].

3.4 Fractographs of alloy under different stress conditions

The typical fractographs of the alloy under typical stress conditions are shown in Figs.6 and 7.

Fig.6 shows that the fractural surfaces consist of three distinct regions, including the region of crack initiation, region of fatigue crack propagation and region of rapid fracture. The radial stripe near the region of crack initiation is more obvious. And then with the crack

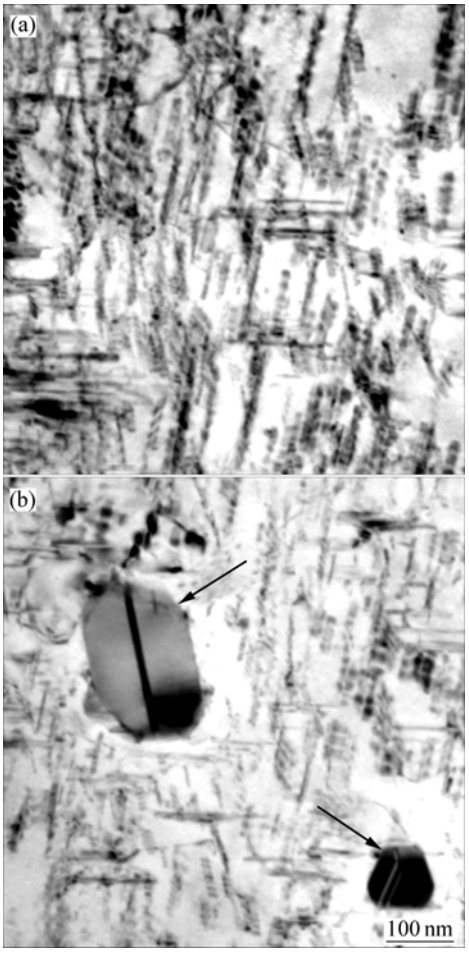

Fig.4 TEM micrographs of 2124-T851 aluminum alloy plane: (a) Precipitated phase *S*; (b) Particles of Al6(Fe, Mn) which are pointed out by arrows

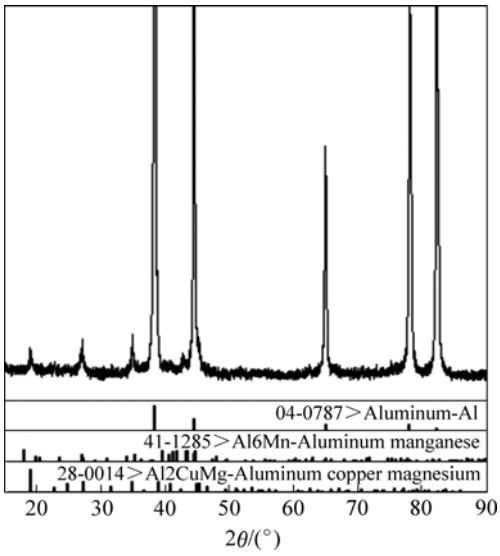

Fig.5 XRD patterns of 2124-T851 aluminum alloy plane

propagating quicker the cracks are gradually sparser. And finally the rapid fracture appears, which is obvious shear lip that looked dimmer than the fatigue crack propagation region. These are due to that the crack tip opening angle becomes greater with the length enlargement of crack, therefore the stress intensity factor *D*-value ΔK increases at the similar stress amplitude condition, which leads to the increase of fatigue crack growth rate. The area of fatigue crack propagation region under lower stress amplitude is bigger than that under the higher one, while the area of rapid fracture region is smaller (Fig.6(a) and Fig.6(b)). At stress of 250 MPa, the region of unstable fatigue crack propagates and the rapid

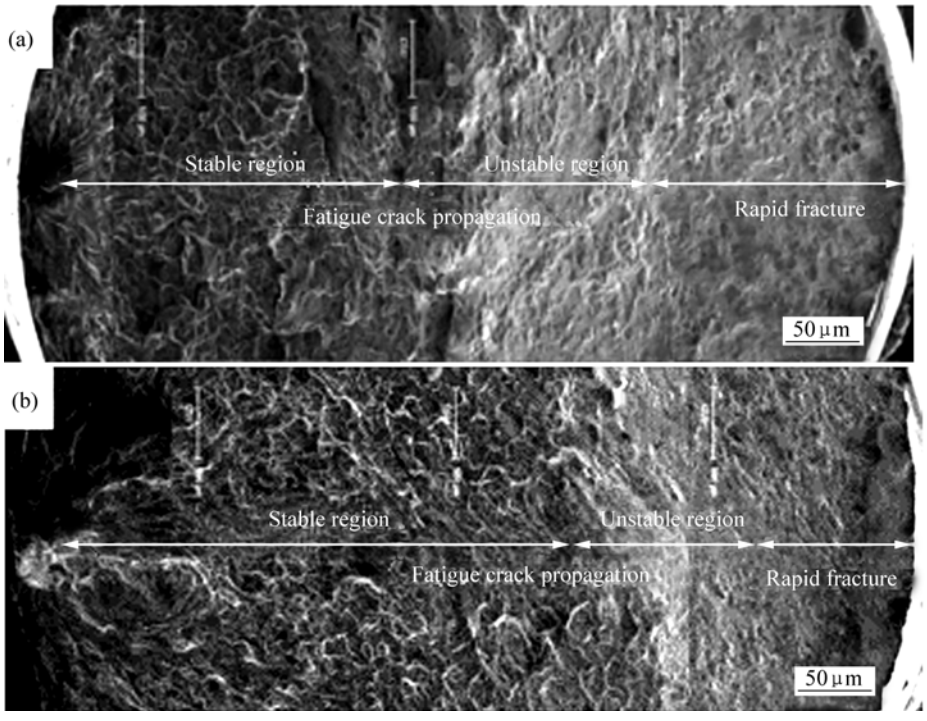

Fig.6 Fractographs of fatigue fracture samples at different stresses amplitude: (a) 400 MPa; (b) 250 MPa

fracture accounts for 2/3 of the whole fracture surface, while 1/2 at stress of 400 MPa.

Fig.7 shows the SEM images of the middle parts of the fatigue crack propagation regions in Fig.6 in which the electron beam is perpendicular to the fracture.

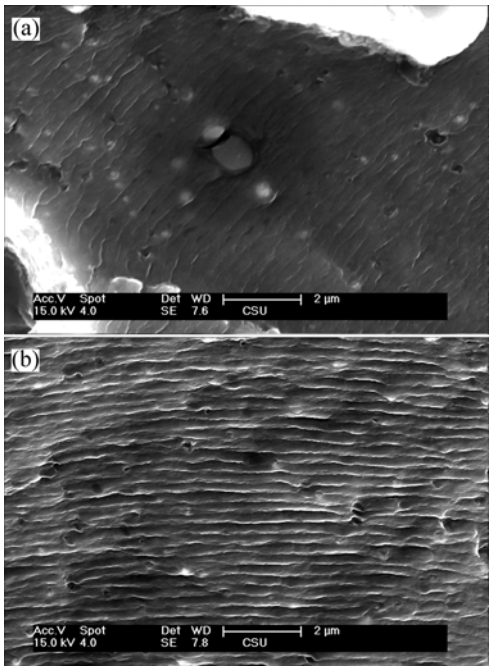

Fig.7 SEM images showing relationship between fatigue fracture characteristic and stress amplitude for 2124-T851 aluminum alloy plate: (a) 400 MPa; (b) 250 MPa

At stress of 400 MPa the width of fatigue striations is 400−500 nm, while about 300 nm at stress of 250 MPa. It shows that the higher the level of stress amplitude is, the wider the width of fatigue striations is, which is coincident with the above results of the corresponding fatigue life tests.

4 Conclusions

1) Under the condition of room temperature and stress ratio R=0.1, the fatigue strength at 10^7 cycles and the fracture toughness of 2124-T851 aluminum alloy with 30 mm in thickness are 243 MPa and 29.6 MPa·$m^{1/2}$, respectively.

2) At high cycle fatigue condition, the higher the stress amplitude, the wider the space between fatigue striations, the faster the rate of fatigue crack developing and going into the intermittent fracture area, and the greater the ratio between the intermittent fracture area and the whole fracture area.

3) The phase structure of 2124-T851 aluminum alloy is composed of the solid solution matrix, dislocation substructure with spot-like precipitated phase S'(Al2CuMg) and Al6(Fe, Mn) particles. During the fatigue testing, the cleavage fracture happens in coarse Al6(Fe, Mn) particles, and this is detrimental to the fatigue properties of the alloy.

References

[1] WANG Chang-zhen, PAN Qing-lin, HE Yun-bin, et al. Effect of heat treatment on microstructure and tensile properties of the thick hot-rolled plate of 2124 aluminum alloy[J]. Mining and Metallurgical Engineering, 2007, 27(1): 68−71.

[2] К У Л Я Ш О Ф В Т. Fracture toughness of aluminum alloys[M]. GAO Zheng-yun. Beijing: Metallurgical Industry Press, 1980: 9. (in Chinese)

[3] LUMLEY R N, POLMEAR I J. The effect of long term creep exposure on the microstructure and properties of an underaged Al-Cu-Mg-Ag alloy[J]. Scripta Materialia, 2004, 50: 1227−1231.

[4] TAN Rong-zhang, WANG Zhu-tang. Aluminum alloy and processing manual[M]. Changsha: Central South University Press, 2005, 2: 221.

[5] TIAN Xiao-feng, FAN Jian-zhong, XIAO Bo-lu, et al. Study on microstructure and mechanical properties of nanocrystalline Al-Cu-Mg alloy[J]. Chinese Journal of Rare Metals, 2007, 31(2): 165−168. (in Chinese)

[6] LIAW P K, GREGGI J G, LOGSDON W A. Microstructure characterization of a silicon carbide whisker reinforced 2124 aluminum metal matrix composite[J]. Journal of Materials Science, 1987, 22(5): 1613−1617.

[7] RAMANATHAN S, KARTHIKEYAN R, KUMAR V DEEPAK, GANESAN G. Hot deformation behavior of 2124 Al alloy[J]. Journal of Materials Science and Technology, 2006, 22(5): 611−615.

[8] WANG S C, STARINK M J. Two types of S phase precipitates in Al-Cu-Mg alloys[J]. Acta Materialia, 2007, 55(3): 933−941.

[9] LIU Hong-jun, LI Ya-min, HAO Yuan. Effect of Al and Cu content on properties of Zn-Al-Cu-Mg alloy[J]. Foundry Technology, 2007, 28(6): 823−826.

[10] SRIVATSAN T S, LANNING DAVID, SONI KAMAL K. Cyclic strain resistance and cyclic fracture behavior of 2124 aluminum alloy[J]. International Journal of Fatigue, 1993, 15(3): 231−242.

[11] KUNG C Y, FINE M E. Fatigue crack initiation and microcrack growth in 2024-T4 and 2124-T4 aluminum alloys[J]. Metall Trans A, 1979, 10(5): 603−610.

[12] ROBIN C, PELLOUX R M. Fatigue crack growth retardation in an aluminum alloy[J]. Mater Sci Eng, 1980, 44(1): 115−120.

[13] CHU Wu-yang. Fracture toughness testing[M]. Beijing: Science Press, 1979: 68−69. (in Chinese)

[14] PAN Qing-ling, HIANG Ji-wu, XUE Song-bai, et al. Metal material science and engineering experimental tutorial[M]. Changsha: Central South University Press, 2006, 9: 85. (in Chinese)

[15] WU Lian-sheng, LIU Zheng-yi. Machinery and equipment failure analysis atlas[M]. Guangdong: Guangdong Science Technology Press, 1990, 10: 219. (in Chinese)

(Edited by CHEN Ai-hua)